Journal of Mathematical Chemistry 25 (1999) 365–382

Solid state reaction kinetics: Structure of the simplest rate–time curve in terms of random tessellations

A. Korobov

Kharkov University, P.O. Box 10313, Kharkov 310023, Ukraine

Received 15 September 1998; revised 19 May 1999

The simplest within the geometric–probabilistic approach rate–time curve is specified and its structure is made explicit in terms of random tessellations. The validity of using the notion of typical cell in this context is verified via direct simulation, and a new description of rate–time curves is suggested. In comparison with the conventional approach this provides a greater scope for exploring chemical regularities of solid state reactions.

1. Introduction: Appearance and essence of rate–time curve

The rate–time curve, result of kinetic experiment and subject of theoretical analysis, is an indispensable tool for exploring chemical reactions of any nature. However, when solid state reactions are concerned, the following essential peculiarity must be taken into account: the form of rate–time curve is determined largely by the universal *geometrical* regularities of first-order phase transitions that always accompany *chemical* transformations under study. The latter thus manifest themselves indirectly. The clear understanding of this goes back to Young [16]. This peculiarity determines a striking contrast between wide variety of solid state reactions, on the one hand, and one and the same form of rate–time curve, on the other hand, and stands in the way of extracting chemical information from experimental data.

In terms of the conventional geometric–probabilistic approach (exposition of which may be found, in particular, in [1,3,4,15]) the only rigorously tractable singular point of the rate–time curve is its maximum which divide it into "front" and "tail". This point corresponds to maximal extension of reaction interface. Along with this, various other parts of the curve are selected more or less arbitrarily. This gives rise to questions which not infrequently remain without substantiated answers.

These questions form part of a wider circle of discrimination issues that was recently discussed in detail in [9–12]. In brief, the conclusion is that to discern chemical regularities through universal geometrical regularities of first-order phase transitions it is necessary (i) to agree geometry of the crystal space of a solid reagent with geometry of phase transitions, and (ii) to take into account geometrical details of the impingements of growing nuclei, which are "avoided" in terms of conventional

formalism. First of these interconnected points received relatively more attention in previous publications. The objective in this paper is to restore the balance through specifying the notion of the simplest rate–time curve and considering its structure in terms of random tessellations.

Any solid state reaction is involved and is fairly seldom mentioned without this attribute. But it means nothing or little without clear reference to something simpler. And not infrequently this is the case when solid state reactions are discussed. Therefore, first of all we need to specify what may serve as an appropriate reference when rate–time kinetic curves are concerned.

For symmetry considerations supported by formal considerations any description of solid state reaction kinetics claiming to represent chemical features must be essentially two-dimensional, geometry of the impingements of growing nuclei being described in terms of random tessellations [11,12]. Among various random tessellations based on nucleation and growth models Voronoi tessellations are the simplest [13,14]. They correspond to the situation when all nuclei are formed at the very beginning of a process. A random tessellation is commonly thought of as a picture obtained after a growth process has been completed. But along with this (static) view another (kinematic) interpretation is also possible. Each cell of a random tessellation may be considered as a "rightful domain" of growing nucleus, and the growth of this nucleus inside the cell may be followed in detail. Impingements with neigbouring nuclei are simulated in these terms as impingements of a nucleus with the edges of its cell. We will restrict ourselves here to the conventional case of linear growth of circular nuclei and will keep usual assumption that the rate is directly proportional to the reaction interface length. This means the possibility to pass from the "rate–time" coordinates to the "interface length–nucleus radius" coordinates. This dependence for a single nucleus within its Voronoi cell will be termed in the present context a primitive kinetic curve (leaving the term "elementary" for what is actually connected with elementary single-barrier acts). The resulting kinetic curve is obviously the sum of primitive curves for all cells of a Voronoi tessellation.

When solid state reactions are described in terms of the geometric–probabilistic approach, no simpler kinetic curve may be specified. Therefore, this curve may be considered as the simplest kinetic curve, and understanding of its structure is necessary as a basis for analysis of more involved cases when nuclei are formed according to more complicated laws, several crystal faces participate in a reaction simultaneously, the limiting stage of a reaction is changed in the course of a process, etc. Within conventional approach this need is far from being satisfied.

2. Direct simulation

Description of solid state reaction kinetics in terms of random tessellations is based essentially on the notion of *typical cell*. For the typical cell of a random Voronoi tessellation a number of characteristics may be calculated analytically; most common are perimeter length, area, and typical edge length [13]. The wide practice of using this

notion in stochastic geometry provides reason enough to expect that it will also work in describing *kinetics* of processes under discussion, i.e., that the primitive kinetic curve constructed for typical cell will provide an acceptable representation of a process as a whole. Various considerations in favour of this were argued previously [9–12]. But still it seems expedient to reinforce this by direct simulation, taking into account that a Voronoi tessellation is a highly correlated construction. In particular, it is necessary to check that doubled distances of edges of a typical cell from its nucleation point will coincide with averaged distances $\langle \delta_k \rangle$ to the nearest, second, etc. nucleation points determined (irrespectively of a Voronoi tessellation) by density function [8]

$$f(\delta_k) = 2(\lambda\pi)^k \big((k-1)!\big)^{-1} \exp\big(-\lambda\pi\delta_k^2\big)\delta_k^{2k-1} \tag{1}$$

and calculated according to the equation

$$\langle \delta_k \rangle = \frac{\Gamma(k+1/2)}{(k-1)!\sqrt{\pi\lambda}}, \tag{2}$$

where λ is the density of nucleation points on the plane, k is the number of a neighbour, and $\Gamma(n)$ is the Euler function.

Also, some additional statistical characteristics necessary in the present context but not available from the literature were estimated.

2.1. Numerical technique and statistical results

A random Voronoi tessellation was estimated in a most direct way (see, for example, [6]):

– An ensemble of 1500 nucleation points was chosen at random. (Proceeding from results obtained in [5] it was concluded that this number of points is sufficient in the present context.)

– All sets of three points were then considered successively. Each such set specifies a circle. If no further point is inside the specified circle, then that circle's center is a vertex of the tessellation.

– After all vertexes were identified in this way, boundary cells were rejected and only internal cells were used for statistical calculations. The ultimate density of nucleation points is 0.93. Thus obtained tessellation is the reciprocal of the Delaunay triangulation associated to the point.

Statistical calculations somewhat more detailed than it is generally accepted were then carried out separately for different ν-gons of the obtained tessellation ($\nu = 3, 4, 5, \ldots$). Along with conventional averaged characteristics (probability p_ν, perimeter length P_ν, area S_ν, typical edge length l_ν) table 1 shows for each value of ν averaged distances to the nearest, second, etc. edges $\langle u_k \rangle$ and averaged lengths of corresponding edges $\langle e_k \rangle$. In the next to last line of the table these characteristics are given for the whole tessellation. The last line contains known analytical

Table 1
Empirical mean values for ν-gons of the random Voronoi tessellation.

ν	p_ν	P_ν	S_ν	l_ν	Averaged distances to edges ($\langle u_k \rangle$)									Averaged lengths of corresponding edges ($\langle e_k \rangle$)								
					1	2	3	4	5	6	7	8	9	1	2	3	4	5	6	7	8	9
3	0.023	2.505	0.287	0.235	0.079	0.17	0.458							0.838	0.92	0.747						
4	0.133	3.644	0.711	0.416	0.198	0.336	0.463	0.668						1.169	0.983	0.836	0.655					
5	0.243	3.856	0.856	0.495	0.213	0.352	0.474	0.621	0.815					1.137	0.947	0.678	0.681	0.413				
6	**0.281**	**4.149**	**1.058**	**0.57**	**0.279**	**0.404**	**0.511**	**0.603**	**0.736**	**0.887**				**1.1**	**0.86**	**0.732**	**0.567**	**0.507**	**0.383**			
7	0.213	4.601	1.313	0.645	0.293	0.424	0.54	0.619	0.747	0.891	1.002			1.208	0.869	0.661	0.56	0.504	0.411	0.389		
8	0.076	5.112	1.689	0.741	0.374	0.518	0.605	0.689	0.783	0.871	0.987	1.003		1.384	0.728	0.774	0.531	0.44	0.587	0.354	0.314	
9	0.023	4.742	1.492	0.716	0.36	0.491	0.539	0.637	0.717	0.794	0.907	0.972	1.023	1.149	1.03	0.316	0.295	0.589	0.356	0.43	0.382	0.194
Whole		**4.178**	**1.075**	**0.559**	**0.263**	**0.395**	**0.511**	**0.63**	**0.767**	**0.884**	**0.994**	**1.083**	**1.076**	**1.161**	**0.897**	**0.711**	**0.594**	**0.477**	**0.42**	**0.392**	**0.332**	**0.355**
Theor.		4.147	1.075	0.591	0.259	0.389	0.486	0.567	0.638	0.702	0.76	0.814	0.865	0.852	0.666	0.52	0.405	0.316	0.246	0.192	0.149	0.116

results: the number of edges of typical cell is 6; the perimeter length $P = 4/\lambda^{1/2}$; the area $S = 1/\lambda$; the typical edge length $l = 2/3\lambda^{1/2}$; averaged distances $\langle u_k \rangle$ are calculated using equation (2); for corresponding edges expected contributions into perimeter length are calculated as

$$\langle e_k \rangle = \frac{1}{\sqrt{\lambda}} \exp\left(-\pi\lambda\langle u_k \rangle^2\right) \tag{3}$$

(see, for example, [2]).

Comparison of such well-known characteristics as the perimeter length and the area with analytical results characterizes in the present context quality of computations which were consciously restricted to relatively small number of nucleation points. The main result is that empirical distances to edges of averaged hexagon coincide well enough with (divided by two) distances calculated using equation (2). At the same time equation (3) gives values which are not in agreement with empirical data and the sum of which is not equal to perimeter length of an averaged cell. This fact, which is most likely connected with non-Gabriel neighbours, is essential in kinetic simulations.

Generally, the straight line joining two neighbouring nuclei may intersect or not intersect the edge between them (figure 1). In the former case these nuclei are termed Gabriel neighbours or full neighbours [13] (e.g., V_0 and V_1 in figure 1). A nucleus may generally have neighbours of both types, and we will term corresponding edges as Gabriel edges (e.g., edge AB in figure 1) and non-Gabriel edges (e.g., edge BC

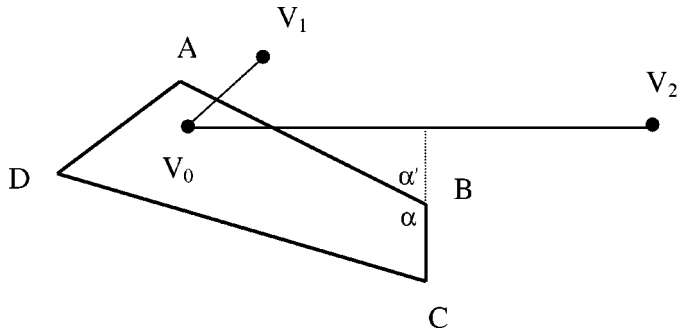

Figure 1. Difference between Gabriel (AB) and non-Gabriel (BC) edges of a cell.

Table 2
Empirical distribution of ν-gons in the number of non-Gabriel edges.

ν	Number of non-Gabriel edges					
	0	1	2	3	4	5
4	0.514	0.486	0	0	0	0
5	0.141	0.391	0.406	0.063	0	0
6	0.054	0.311	0.365	0.23	0.041	0
7	0.018	0.089	0.232	0.339	0.251	0.07
8	0	0	0.19	0.26	0.49	0.06

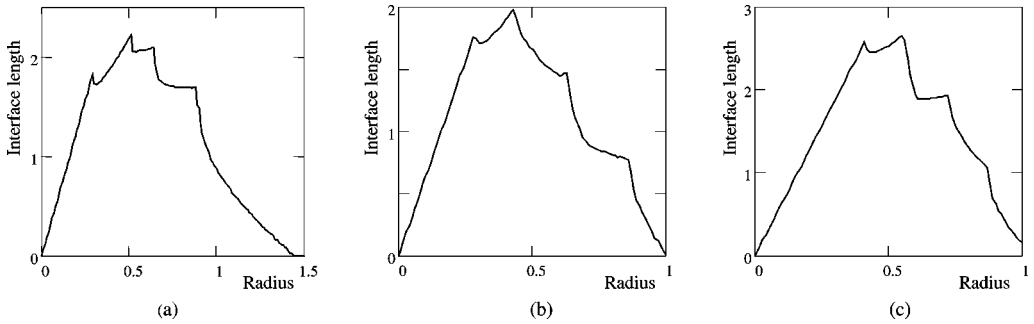

Figure 2. Examples of primitive kinetic curves obtained by direct simulation.

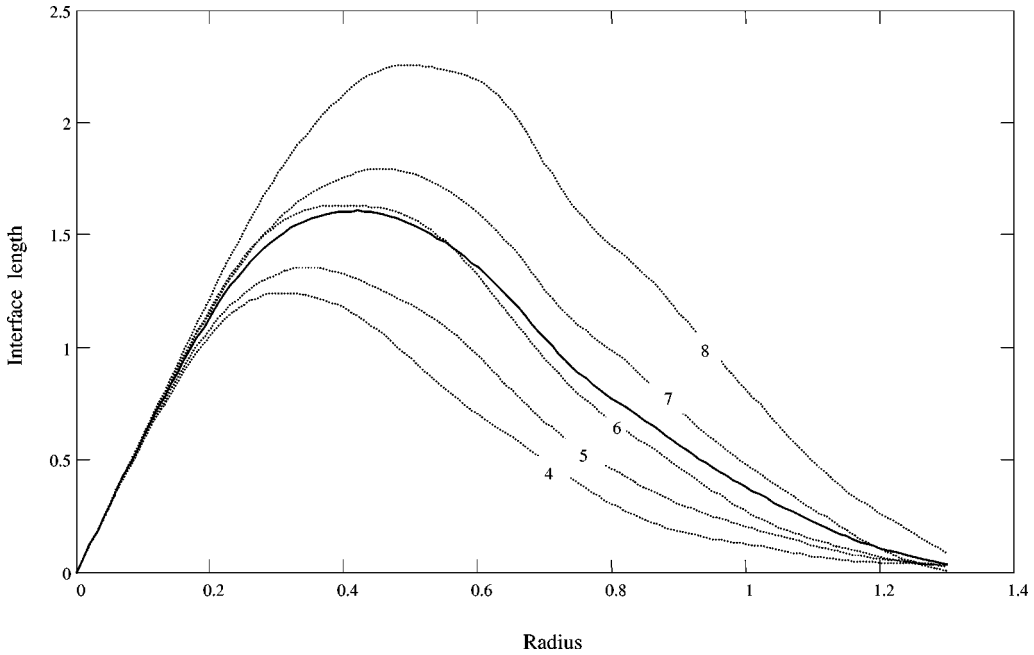

Figure 3. The simplest kinetic curve for the whole tessellation obtained by direct simulation (solid) in comparison with kinetic curves for different ν-gons ($\nu = 4, 5, 6, 7, 8$) of this tessellation (dot lines).

in figure 1). The present study shows that non-Gabriel edges considerably prevail. Moreover, ν-gons of the tessellation are distributed in a regular manner in the number of non-Gabriel edges (table 2). This result will be essentially used below.

2.2. The simplest kinetic curve as the sum of primitive curves

For a direct simulation of the processes of growth and impingements the program of statistical analysis was adapted for computing the primitive kinetic curve for each cell of the tessellation. For $0 \leqslant r \leqslant h_\nu$ (where h_ν is the distance to the most distant

vertex) a series of concentric circles with the nucleation point of a cell as a center was constructed, and that part which fit into the cell was then determined for each circle. Figure 2 shows some of primitive kinetic curves obtained in this way. The simplest kinetic curve under discussion is nothing else but the sum of primitive curves for all cells of the tessellation. This sum (divided by the number of cells) is shown in figure 3 together with sums calculated in the same way separately for 4-, 5-, 6-, 7- and 8-gons. This figure provides a visual evidence that the averaged curve for 6-gons provides a good approximation of the averaged curve for the whole tessellation. Note that maximum of each curve coincides with the averaged distance to the second edge of corresponding ν-gon (cf. table 1).

By and large, above results make it possible to conclude that in simulating kinetics of growth and impingement processes there are good grounds to consider the typical hexagonal cell as a "plenipotentiary" of random tessellation as a whole.

3. A kinematic portrait of the simplest kinetic curve step-by-step

Now we are in a position to construct the simplest kinetic curve step-by-step and thus to get an insight into its structure. We will need the following simple geometrical relationships. If the growth of a circular nucleus is restricted with one straight line (figure 4(a)), dependence of perimeter length w on nucleus radius r may be represented as

$$w(r) = r\left(2\arcsin\left(\frac{u}{r}\right) + \pi\right), \tag{4}$$

where u is the distance of a circle's center from the restriction line. If the growth is restricted with two lines forming an angle α, then

$$w(r) = r\left(\arcsin\left(\frac{u_1}{r}\right) + \arcsin\left(\frac{u_2}{r}\right) \pm \alpha\right), \tag{5}$$

where "$+$" before α corresponds to the situation shown in figure 4(b) (growth outside) and "$-$" corresponds to the situation shown in figure 4(c) (growth inside). If growth

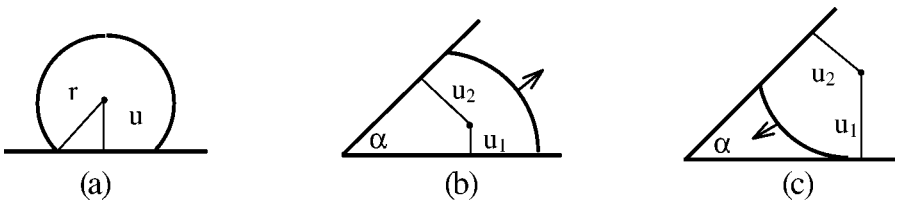

Figure 4. Growth of a circular nucleus restricted with one (a) and two (b, c) straight lines.

proceeds in both directions then

$$w(r) = 2r\left(\arcsin\left(\frac{u_1}{r}\right) + \arcsin\left(\frac{u_2}{r}\right)\right). \tag{6}$$

The same equation holds when growth is restricted by two parallel lines.

3.1. Restriction with one straight line

This is the simplest model situation which provides an idea of the approach suggested.

If the growth of a circular nucleus is restricted with one straight line, then the equation of primitive kinetic curve for this nucleus reads

$$w(r,u) = \begin{cases} 2\pi r, & r \leqslant u, \\ r\left(2\arcsin\left(\dfrac{u}{r}\right) + \pi\right), & r \geqslant u. \end{cases} \tag{7}$$

For an ensemble of nuclei with distances u from the restriction line being distributed according to equation (1) the "observed" kinetic curve $W(r)$ may be represented as an integral

$$W(r) = \int_0^\infty w(r,u) f(u)\,\mathrm{d}u = 2\pi r - 4\pi\lambda r \int_0^r \arccos\left(\frac{u}{r}\right) \exp\left(-\lambda\pi u^2\right) u\,\mathrm{d}u. \tag{8}$$

This curve is shown in figure 5 together with primitive curve $f(r, \langle u\rangle)$ for the averaged distance $\langle u\rangle$ calculated using equation (2). We see that this primitive curve provides

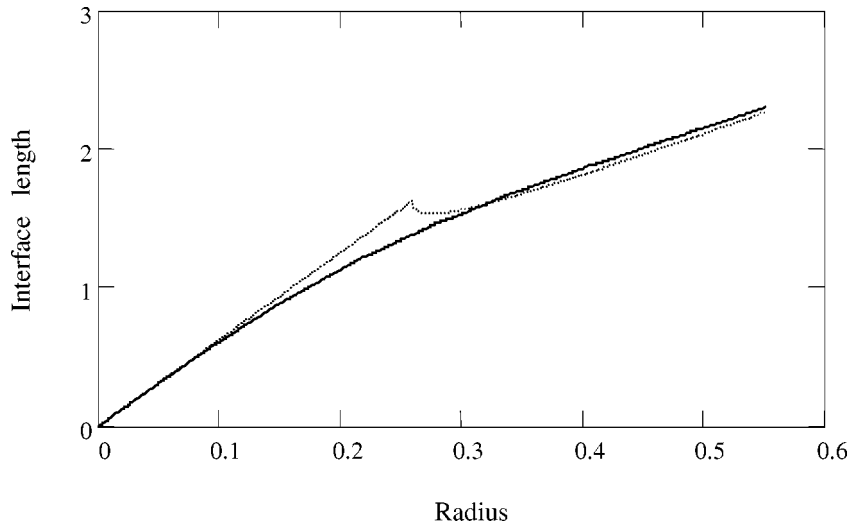

Figure 5. Nucleus growth is restricted with one straight line: "observed" kinetic curve (solid) in comparison with primitive curve (dot) calculated for the averaged distance.

a fairly good representation of the "observed" curve $W(r)$. In particular, its peak indicates a characteristic point of $W(r)$ curve, the point of maximal curvature.

3.2. Restriction with two straight lines: appearance of maximum

This model situation enables one to follow appearance of the maximum on a kinetic curve and to pass to the general case. Restriction lines may be parallel or may form an angle; in the latter case nucleus radius r must be less than distance h to the angle.

When there are two (or more) restriction lines, the equation of primitive kinetic curve may be represented in two different ways. If no restrictions are posed on u_1 and u_2, then

$$w(r,u_1,u_2)=\begin{cases}2\pi r, & r\leqslant u_1 \text{ and } r\leqslant u_2,\\ r\left(2\arcsin\left(\dfrac{u_1}{r}\right)+\pi\right), & u_1\leqslant r\leqslant u_2,\\ r\left(2\arcsin\left(\dfrac{u_2}{r}\right)+\pi\right), & u_2\leqslant r\leqslant u_1,\\ 2r\left(\arcsin\left(\dfrac{u_1}{r}\right)+\arcsin\left(\dfrac{u_2}{r}\right)\right), & r\geqslant u_1 \text{ and } r\geqslant u_2.\end{cases} \tag{9}$$

An alternative possibility is connected with the need to distinguish explicitly distances to the nearest, second, etc. restriction lines. Then $u_1<u_2$ and

$$w(r,u_1,u_2)=\begin{cases}2\pi r, & r\leqslant u_1,\\ r\left(2\arcsin\left(\dfrac{u_1}{r}\right)+\pi\right), & u_1\leqslant r\leqslant u_2,\\ 2r\left(\arcsin\left(\dfrac{u_1}{r}\right)+\arcsin\left(\dfrac{u_2}{r}\right)\right), & r\geqslant u_2.\end{cases} \tag{10}$$

Since this is the case in the present context, the second form will be used. Accordingly, it will be assumed throughout that u_1 always denotes the distance to the nearest restriction line, u_2 always denotes the distance to the second restriction line, etc., i.e., $u_1<u_2<u_3<\cdots$. This is in agreement with the form in which density function (1) is specified.

Integration with respect to u_1 and u_2 distributed according to equation (1) gives

$$W(r)=2r\left[\pi-\int_0^r \arccos\left(\frac{u_1}{r}\right)f(u_1)\,\mathrm{d}u_1 - \int_0^r\int_0^r \arccos\left(\frac{u_2}{r}\right)f(u_1)f(u_2)\,\mathrm{d}u_1\mathrm{d}u_2\right]. \tag{11}$$

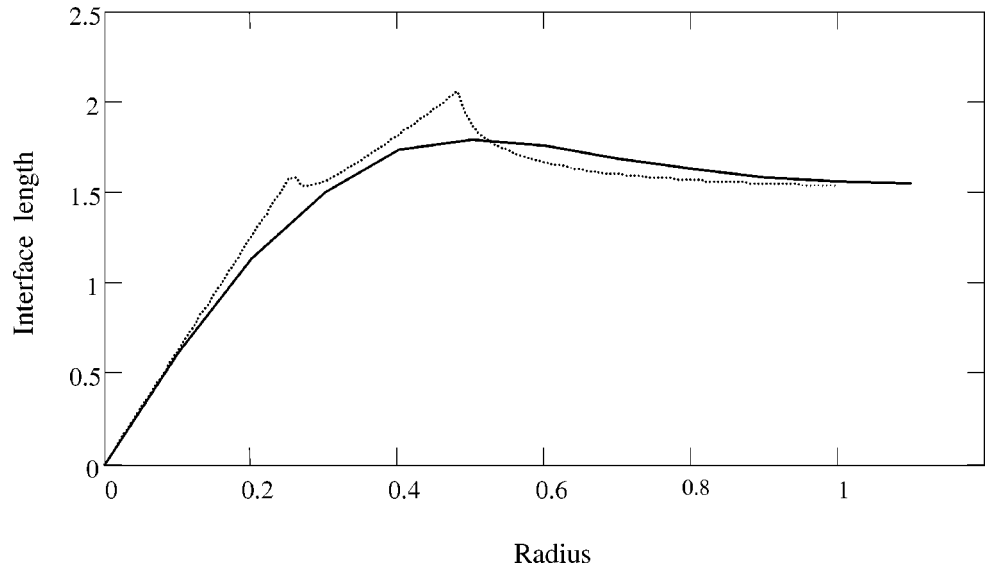

Figure 6. Nucleus growth is restricted with two straight lines: "observed" kinetic curve (solid) in comparison with primitive curve (dot) calculated for the averaged distances.

Curves $W(r)$ and $w(r, \langle u_1 \rangle, \langle u_2 \rangle)$ are compared in figure 6: the maximum of $W(r)$ curve corresponds to $\langle u_2 \rangle$. We will see that this regularity is preserved in passing to greater number of restriction lines.

3.3. General equation of primitive kinetic curve

In reality the growth of nuclei is restricted by closed ν-gons of a random tessellation. Each ν-gon is characterized by an "urchin", a ν-dimensional vector **u** of distances from the nucleation point to cell edges, and a "hedgehog", a ν-dimensional vector **h** of distances from the nucleation point to cell vertexes. When in the course of growth the radius of a nucleus becomes equal to any of u_i or h_i, the dynamics of growth is changed. Accordingly, equation of the primitive kinetic curve for a ν-gon similar to equations (7) and (10) consists of 2ν analytical expressions.

The whole spectrum of primitive kinetic curves for a given ν may be described with the use of a $(0, 1)$-matrix K of the form

$$K = (U\ H), \tag{12}$$

where U is a submatrix describing the situation of a growing nucleus with respect to edges, and H is a submatrix describing its situation with respect to vertexes. Submatrix U may be constructed in the following way. Take the set $\{1, 2, \ldots, \nu\}$ and form the set S of all its subsets. Each of 2^ν elements of S determines a row of a matrix U_0 according to the simple rule: it indicates elements that have unit values; all other

elements have zero values. For example, element 24 of S indicates that second and fourth elements in a row have unit values; if, for instance, $\nu = 6$ then this row is $\{0\,1\,0\,1\,0\,0\}$.

Matrix U_0 represents the complete combinatorics of edges without regard for vertexes. Submatrix H is constructed proceeding from U_0. One and the same row of U_0 may generate more than one row of H. If so, this row of U_0 is repeated, and ultimately one gets submatrix U. In other words, submatrix U consists of the same rows as U_0 some of which are repeated. A row of submatrix H may contain 0 to $k-1$ unit elements where k is the number of unit elements in generating row of U_0. Zero row of H corresponds to each row of U_0. If $k \geqslant 2$, further rows of H are constructed in the following way. If the ith element in a row of U_0 has the unit value and the next element also has the unit value, the ith element of corresponding row of H is assigned the unit value. (The first element in a row of U_0 is considered as the next to the last element.) Then these basic rows, each of which contains one unit element, are added in all possible combinations (pairwise, triplewise, etc.) to give new rows of H for which the generating row of U_0 is also repeated. The result is matrix K describing the whole spectrum of primitive kinetic curves. To save the room, the transposed matrix for $\nu = 3$ is shown below:

$$\begin{pmatrix}
0 & 0 & 0 & 0 & 0 & 0 & 0 & 1 & 0 & 0 & 0 & 0 & 0 & 1 & 0 & 1 & 1 & 1 \\
0 & 0 & 0 & 0 & 0 & 0 & 0 & 0 & 0 & 1 & 0 & 0 & 1 & 0 & 1 & 0 & 1 & 1 \\
0 & 0 & 0 & 0 & 0 & 1 & 0 & 0 & 0 & 0 & 0 & 1 & 0 & 0 & 1 & 1 & 0 & 1 \\
0 & 0 & 0 & 1 & 0 & 0 & 1 & 1 & 1 & 1 & 1 & 1 & 1 & 1 & 1 & 1 & 1 & 1 \\
0 & 0 & 1 & 0 & 1 & 1 & 0 & 0 & 1 & 1 & 1 & 1 & 1 & 1 & 1 & 1 & 1 & 1 \\
0 & 1 & 0 & 0 & 1 & 1 & 1 & 1 & 0 & 0 & 1 & 1 & 1 & 1 & 1 & 1 & 1 & 1
\end{pmatrix}.$$

Each of its columns (i.e., each row of matrix K) corresponds to a definite situation of a growing nucleus with respect to edges and vertexes of a ν-gon. For example, the sixth row means that two edges and the angle between them are reached by a growing nucleus.

For a particular ν-gon with given set $\mathbf{p} = \{u_1, \ldots, u_\nu,\ h_1, \ldots, h_\nu\}$ and all edges being Gabriel the primitive kinetic curve $w(r, \mathbf{p})$ is calculated in the following way. Radius r of a growing nucleus goes through $[0, h_\nu]$ interval with an appropriate step. For each value of r a row i of matrix K is chosen such that $\widetilde{K}_{ij}(r - p_j)$ for all $1 \leqslant j \leqslant 2$; $\widetilde{K}$ is a matrix obtained from K by replacing all zero elements by -1. This row is unique and determines one of 2ν analytical expressions describing corresponding primitive curve:

$$w_i(r, p) = r\left[K_i R + \left(2 - \sum_{j=1}^{\nu} K_{ij}\right)\pi\right], \tag{13}$$

where R is a restriction vector in which top ν elements correspond to equation (4)

(within π which is taken into account in equation (13)) and other elements correspond to equation (5) (within the sign):

$$R = \begin{pmatrix} 2\arcsin\left(\frac{u_1}{r}\right) \\ \vdots \\ 2\arcsin\left(\frac{u_\nu}{r}\right) \\ \arcsin\left(\frac{u_1}{h_1}\right) + \arcsin\left(\frac{u_2}{h_1}\right) - \arcsin\left(\frac{u_1}{r}\right) - \arcsin\left(\frac{u_2}{r}\right) \\ \vdots \\ \arcsin\left(\frac{u_i}{h_i}\right) + \arcsin\left(\frac{u_{i+1}}{h_i}\right) - \arcsin\left(\frac{u_i}{r}\right) - \arcsin\left(\frac{u_{i+1}}{r}\right) \\ \vdots \\ \arcsin\left(\frac{u_\nu}{h_\nu}\right) + \arcsin\left(\frac{u_1}{h_\nu}\right) - \arcsin\left(\frac{u_\nu}{r}\right) - \arcsin\left(\frac{u_1}{r}\right) \end{pmatrix}. \quad (14)$$

Transition to another row of matrix K occurs each time when r becomes equal to one of u_k or h_k.

If an $(i+1)$th edge of a ν-gon is non-Gabriel (the nearest edge cannot be non-Gabriel), then the corresponding row of vector R

$$\arcsin\left(\frac{u_i}{h_i}\right) + \arcsin\left(\frac{u_{i+1}}{h_i}\right) - \arcsin\left(\frac{u_i}{r}\right) - \arcsin\left(\frac{u_{i+1}}{r}\right) \quad (15)$$

is replaced by

$$\arcsin\left(\frac{u_i}{h_i}\right) + \pi - \arcsin\left(\frac{u_{i+1}}{h_i}\right) - \arcsin\left(\frac{u_i}{r}\right) - \arcsin\left(\frac{u_{i+1}}{r}\right) \quad (16)$$

and the value of u_{i+1} is replaced in **p** by the value of h_{i+1}. This means (see figure 1) that complementary angle α' is taken instead of α and dynamics of growth is not changed until this vertex is reached.

In this way any possible primitive kinetic curve may be constructed; in particular, curves shown in figure 2 may be reproduced.

3.4. 6-gons: a kinematic portrait of typical cell

The next step is to construct the primitive curve for the typical cell of random Voronoi tessellations as described in the previous subsection and to check whether or not it is capable of representing the "observed" curve obtained above by direct simulation. But at this stage we face the fact that available information about the

Table 3
Characteristics of the typical cell.

i	% of non-Gabriel	$\langle u_i \rangle$	$\langle h_i \rangle$
1	0	0.279	0.493
2	20.3	0.404	0.602
3	31.1	0.511	0.682
4	36.5	0.603	0.797
5	47.3	0.736	0.926
6	54.1	0.887	1.019

typical cell is insufficient for this and some additional statistical characteristics are required.

An attempt to find out a most typical mutual situation of the nearest, second, etc. edges failed: practically all 60 possibilities for 6-gons are present in the tessellation with fairly close frequencies.

Nevertheless, a peculiar sequence of edges exists and is determined by the statistics of non-Gabriel edges. Table 3 shows the percentage of non-Gabriel edges among the nearest, second, etc. edges of 6-gons. Note that the nearest edge cannot be non-Gabriel at all and that from two adjacent edges only more distant from the nucleation point may be non-Gabriel with respect to less distant. It follows that the sequence of edges $\{1, 2, 3, 4, 5, 6\}$ is the only sequence suitable for representing statistical characteristics of typical cell specified in table 3: for any other permutation at least two edges will be completely Gabriel. These considerations are supported by empirical averaged distances to the nearest, second, etc. vertexes (table 3) which alternate with corresponding distances to edges:

$$\langle u_1 \rangle < \langle u_2 \rangle < \langle h_1 \rangle < \langle u_3 \rangle < \langle h_2 \rangle < \langle u_4 \rangle < \langle h_3 \rangle < \langle u_5 \rangle < \langle h_4 \rangle < \langle u_6 \rangle < \langle h_5 \rangle < \langle h_6 \rangle. \tag{17}$$

The primitive kinetic curve constructed for the typical averaged hexagon possessing the above characteristics, i.e., the hexagon the nearest edge of which is completely Gabriel, the second edge is 20.3% non-Gabriel, the third edge is 31.1% non-Gabriel, etc., is shown in figure 7 together with the "observed" curve reproduced from figure 3. It may be considered as a kinematic portrait of the typical cell or of the simulated curve, and we may conclude that this portrait provides a good representation of the original except a distant part of the tail.

3.5. Front and tail of the simplest kinetic curve

We see that an obvious "asymmetry" exists in describing the simplest kinetic curve in terms of random tessellations: whereas for the distances to edges we may use density function (1) (one of relatively few relevant density functions for which analytical expression is known), for the distances to vertexes we possess only empirical

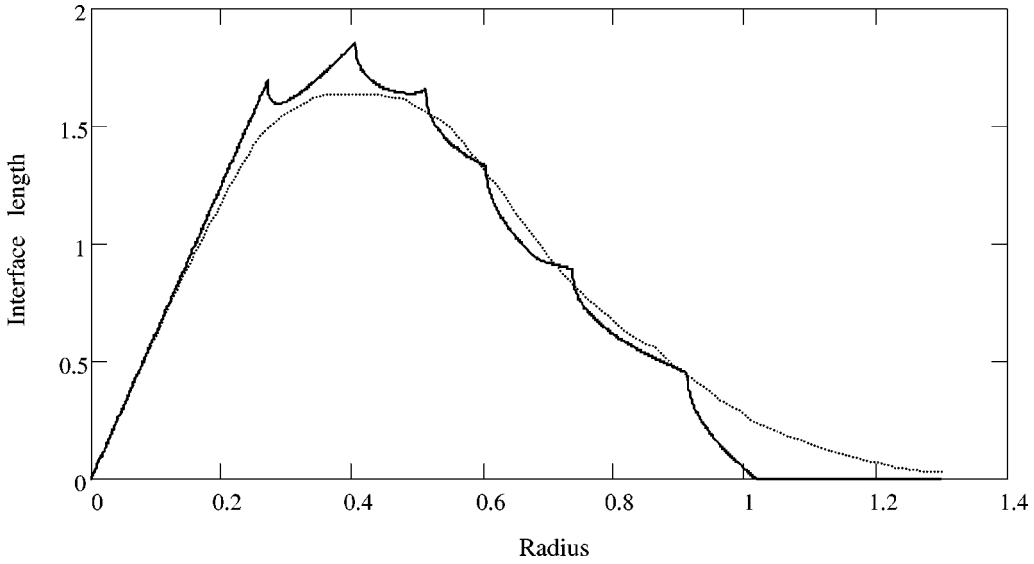

Figure 7. Primitive kinetic curve for the typical cell (solid) in comparison with the "observed" curve (dot) reproduced from figure 3.

information. Accordingly, it is reasonable to consider possible approximations for the latter.

First consider the situation when distance to the nearest vertex exceeds that to the most distant edge. It is clear from the above statistical data that this approximation is fairly artificial. But nevertheless, it enables one to get a keener insight into the structure of the simplest curve: since within this approximation all edges are reached by a growing nucleus before the first vertex, the multiple integral

$$I(r) = \int_0^\infty \dots \int_0^\infty w(r, u_1, \dots, u_n) f(u_1) \cdots f(u_n)\, \mathrm{d}u_1 \dots\, \mathrm{d}u_n \tag{18}$$

may be represented as

$$\begin{aligned} I(r) &= 2r \left[\pi - \int_0^r \arccos\left(\frac{u_1}{r}\right) f(u_1)\, \mathrm{d}u_1 \right. \\ &\quad \left. - \int_0^r \int_0^r \arccos\left(\frac{u_2}{r}\right) f(u_1) f(u_2)\, \mathrm{d}u_1\, \mathrm{d}u_2 - \cdots \right] \\ &= 2r\left[\pi - I_1(r) - I_2(r) - \cdots - I_n(r)\right] = 2r\left(\pi - \sum_{k=1}^{n} I_k(r)\right). \end{aligned} \tag{19}$$

If we restrict ourselves to $I_1(r)$ only, this will correspond to the restriction of growth by one straight line, etc. Figure 8(a) shows four $I(r)$ curves calculated for $n = 1, 2, 3$ and 4 in comparison with the "observed" curve. Starting from $n = 2$ they provide a good approximation to the front of simulated curve; the point at which they are split

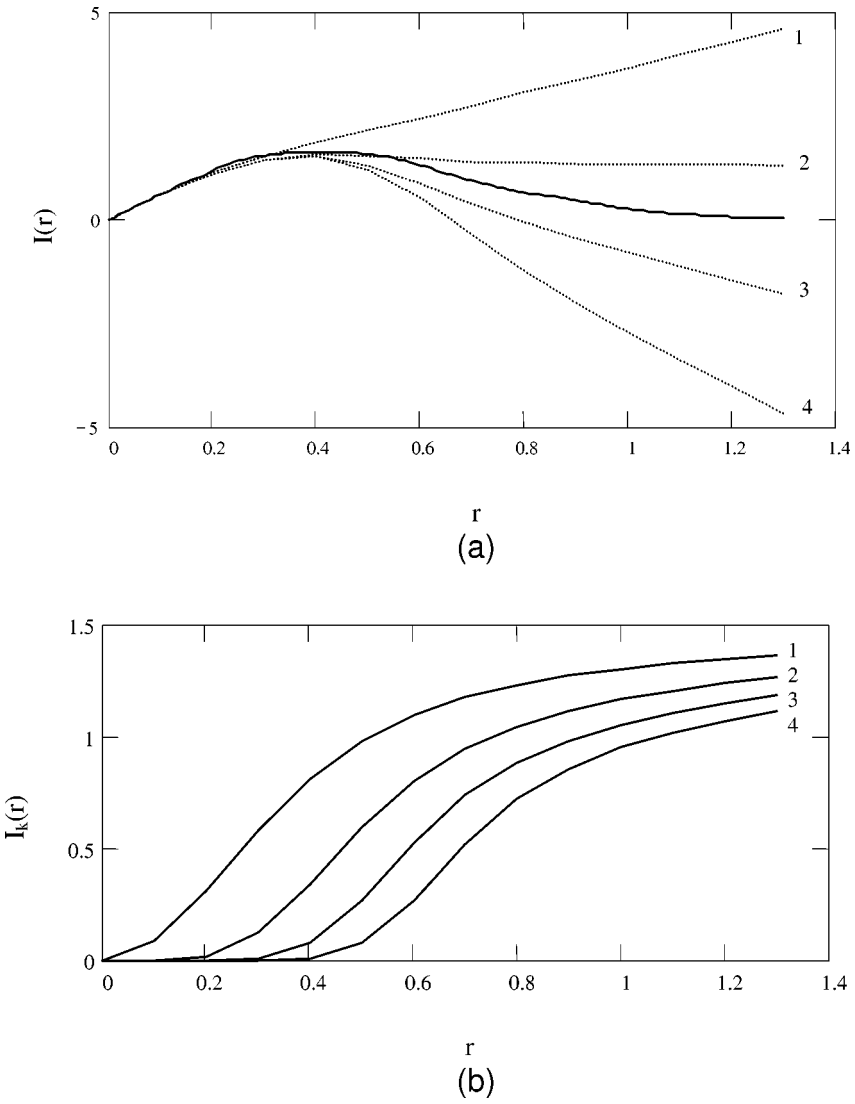

Figure 8. (a) Integral curves calculated using equation (18) for $n = 1, 2, 3$ and 4 (dot) in comparison with the "observed" curve (solid) reproduced from figure 3; (b) corresponding $I_k(r)$ integrals for $k = 1, 2, 3$ and 4.

into a bunch corresponds to its maximum. For $n = 1$ approximation is satisfactory within $[0, \langle u_1 \rangle]$ interval. Figure 8(b) shows corresponding $I_k(r)$ integrals. We see that at $r \leqslant \langle u_2 \rangle$ the contribution of $I_3(r)$ into $I(r)$ is sufficiently small and that of $I_4(r)$ is practically negligible. This picture demonstrates that front of the simplest kinetic curve is simpler in a sense than its tail: front is determined mainly by edges of random cells (largely by two first edges one of which cannot be non-Gabriel at all) whereas behaviour of tail depends on greater number of factors and is essentially determined

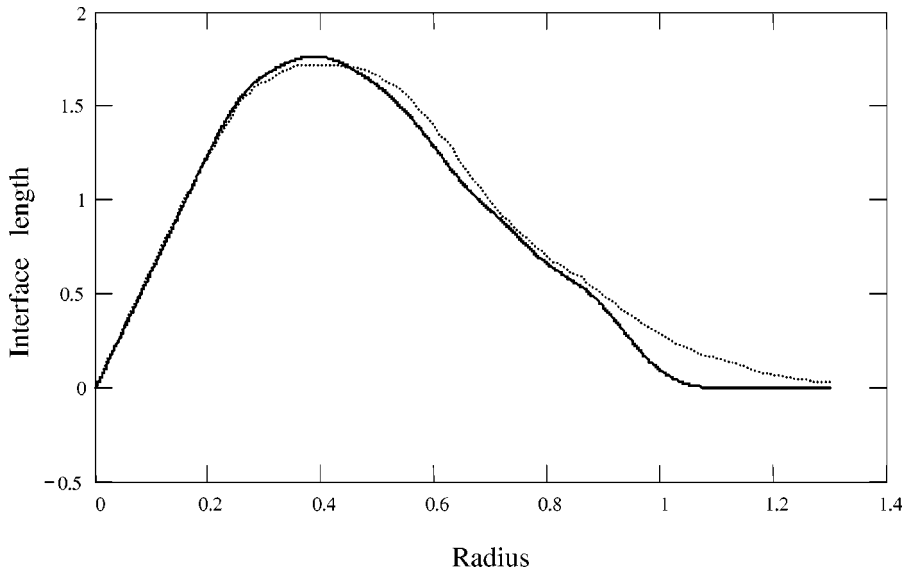

Figure 9. Smoothed primitive kinetic curve for the averaged hexagon (solid) in comparison with the "observed" curve (dot) reproduced from figure 3.

by vertexes. This means that in contrary to tail front may be simulated in a relatively simple way.

Much more adequate approximation is to calculate averaged distances to vertexes of the typical hexagon with the account of inequality (17) as arithmetic mean

$$h_i = \begin{cases} \dfrac{u_{i+1} + u_{i+2}}{2}, & i = 1, 2, 3, 4, \\ \dfrac{3u_6 - u_5}{2}, & i = 5, \\ 2u_6 - u_5, & i = 6, \end{cases} \tag{20}$$

where $\langle u_i \rangle$ are calculated using equation (2). Then the primitive kinetic curve may be constructed for the hexagon with these characteristics as described above. Parameters p_i for this primitive curve are easy to calculate, and therewith it does not differ essentially from the curve shown in figure 7. A further possible step is to apply one of conventional smoothing procedures to this piecewise curve. As a result one arrives at a fairly good approximation of the simulated curve (figure 9). This figure was obtained with the use of the symmetric k-nearest neighbour linear least square fitting procedure [7]. But several other tested common procedures also proved to be suitable. This technique is new for solid state reaction kinetics and seems to be promising for further development of kinetic analysis.

4. Conclusions

Epithet “the simplest” means in the present context that no simpler alternative exists within the geometric–probabilistic approach to solid state reaction kinetics. However, above considerations show that even the simplest kinetic curve under discussion is not at all simple. The main conclusions concerning it may be summarized as follows.

(1) The simplest kinetic curve is a function which describes the growth and impingements of two-dimensional nuclei that are formed simultaneously at the very beginning of a process on a single crystal face.

(2) In conventional terms of coverings this curve is “structureless” because of the fact that geometrical details of nuclei impingements are avoided within this approach. Its structure becomes explicit in terms of tessellations due to the possibility of taking these details into account.

(3) In describing the simplest kinetic curve in terms of random tessellations the typical cell is shown to be representative enough. The distances from the nucleation point to cell edges may be calculated using equation (1) which means the possibility to use one of few relevant density functions for which analytical expression is known.

(4) A reasonable approximation of the simplest kinetic curve may be obtained by smoothing the primitive kinetic curve constructed for typical cell. This technique is new for solid state reaction kinetics and may appear to be useful in setting and solving inverse kinetic problems (IKP).

(5) The simplest kinetic curve is subdivided by its maximum into front and tail. In terms of tessellations front is simpler than tail and may be described in a relatively simple way. This may be sufficient when the curve is analyzed as itself or in the context of a relatively simple IKP. In the case of relatively complicated IKP tail also may be involved into analysis, but this requires more laborious calculations with the use of empirical data.

References

[1] P. Barret, *Cinétique Hétérogene* (Gauthier-Villars, Paris, 1973).
[2] V.Z. Belen’kiy, *Geometric–Probabilistic Models of Crystallization* (Nauka, Moscow, 1980) (in Russian).
[3] M.E. Brown, D. Dollimore and A.K. Galwey, *Reactions in the Solid State* (Elsevier, Amsterdam, 1980).
[4] B. Delmon, *Introduction á la Cinétique Hétérogene* (Éditions Technip, Paris, 1969).
[5] J.M. Drouffe and C. Itzykson, Nuclear Phys. B 235 (1984) 45.
[6] H.J. Frost and C.V. Thompson, Acta Metall. 35 (1987) 529.
[7] N. Kalitkin, *Numerical Methods* (Nauka, Moscow, 1978) (in Russian).
[8] M.G. Kendall and P.A.P. Moran, *Geometrical Probabilities* (Griffin and Co, London, 1963).
[9] A. Korobov, Thermochim. Acta 243 (1994) 79.

[10] A. Korobov, J. Math. Chem. 17 (1995) 323.
[11] A. Korobov, Heterogeneous Chem. Rev. 3 (1996) 477.
[12] A. Korobov, Geometrical probabilities in heterogeneous kinetics: 60 years of side by side development, J. Math. Chem. 24 (1998) 261.
[13] J. Møller, *Lectures on Random Voronoi Tessellations*, Lecture Notes in Statistics, Vol. 87 (Springer-Verlag, New York, 1994).
[14] A. Okabe, B. Boots, K. Sugihara and S.N. Chiu, *Spatial Tessellations: Concepts and Applications of Voronoi Diagrams* (Wiley, New York, 1999).
[15] J. Šestak, *Thermophysical Properties of Solids, Their Measurements and Theoretical Thermal Analysis* (Elsevier, Amsterdam, 1984).
[16] D. Young, *Decomposition of Solids* (Pergamon Press, 1966).